# Star Formation History in the Central Region of the Barred Galaxy NGC 7177

## O. K. Sil'chenko[1*] and A. A. Smirnova[2]

[1]*Sternberg Astronomical Institute, Universitetskii pr. 13, Moscow, 119992 Russia*
[2]*Special Astrophysical Observatory, Russian Academy of Sciences,*
*Nizhnii Arkhyz, Karachai-Cherkessian Republic, 369167 Russia*
Received May 18, 2009

**Abstract**—Using the method of two-dimensional spectroscopy, we have investigated the kinematics and distribution of the gas and stars at the center of the early-type spiral galaxy NGC 7177 with a medium-scale bar as well as the change in the mean age of the stellar population along the radius. A classical picture of radial gas inflow to the galactic center along the shock fronts delineated by dust concentration at the leading edges of the bar has been revealed. The gas inflow is observed down to a radius $R = 1''.5-2''$, where the gas flows at the inner Lindblad resonance concentrate in an azimuthally highly inhomogeneous nuclear star formation ring. The bar in NGC 7177 is shown to be thick in $z$ coordinate—basically, it has already turned into a pseudo-bulge as a result of secular dynamical evolution. The mean stellar age inside the star formation ring, in the galactic nucleus, is old, $\sim 10$ Gyr. Outside, at a distance $R = 6''-8''$ from the nucleus, the mean age of the stellar population is $\sim 2$ Gyr. If we agree that the bar in NGC 7177 is old, then, obviously, the star formation ring has migrated radially inward in the last $1-2$ Gyr, in accordance with the predictions of some dynamical models.

## INTRODUCTION

In recent years, the understanding that slow dynamical processes can play a very important role, to the extent that they can change radically the global morphology of galaxies on time scales of $1-5$ Gyr, has matured among the researchers of galactic evolution. Such slow processes have been collectively called "secular evolution". They include both the internal instabilities of dynamically cold stellar disks and the processes related to the gravitational interaction with neighboring galaxies and to the hydrodynamic interaction with the intergalactic medium. A good comprehensive review of the present views of secular galactic evolution has recently been published by Kormendy and Kennicutt (2004). Interestingly, most of the secular evolution mechanisms redistribute the matter in galaxies in such a way that the gas from the outer galactic disk regions flows into the central region and star formation can and must take place there, leading to the formation of new stellar subsystems: pseudo-bulges, chemically decoupled stellar nuclei, young ring structures, etc.

NGC 7177 is a medium-luminosity Sb-type spiral galaxy with a well-developed medium-sized bar (Fig. 1). The nucleus of NGC 7177 is a weak LINER (Misselt et al. 1999). The peculiarities of this galaxy make it a convenient object for investigation, which is also confirmed by the fact that NGC 7177 has been repeatedly included in the samples of both photometric and kinematic surveys. Photometric information about the structure of NGC 7177 can be found in de Jong (1996). Analyzing the galaxy's CCD images in several color bands based on the standard "exponential disk plus de Vaucouleurs bulge" model, de Jong discovered a compact bulge ($r_e = 7''$), a small ($h = 13'' (K) - 11'' (B)$ or about 1.5 kpc) dense stellar disk with a surface brightness that is approximately triple the standard one ($\mu_{0,B} = 20^m.46$ arcsec$^{-2}$), and a bar with a radius of $13''$ oriented at a position angle of $13° (K$ band)$-18° (B$ band) in NGC 7177. Erwin (2005) refined the photometric parameters of the galaxy: the bar radius is $10''-11''$ and the disk orientation in space estimated from the shape of its outer isophotes by assuming the disk to be circular is: the inclination $48°$ and the position angle of the line of nodes $PA_0 = 83°$. Erwin et al. (2008) analyzed the radial surface
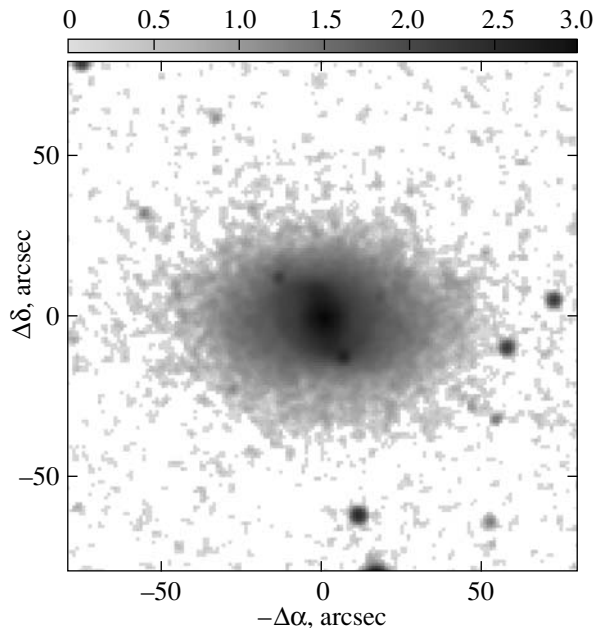
*E-mail: olga@sai.msu.su

**Fig. 1.** Image of NGC 7177 from 2MASS data, the sum of three infrared bands $J + H + K_s$. The intensity scale is logarithmic, with an arbitrary zero point; north is at the top and east is to the left.

brightness profile for NGC 7177 based on a deeper $R$-band image without obsessing about the concept of single-exponential disks. They discovered another outer stellar disk that begins to dominate in the galactic structure at a distance of 89″ (about 7 kpc) from the center; this disk has a large scale length, 84″ (about 7 kpc), and a low surface brightness, $\mu_{0,R} = 23^m5$ arcsec$^{-2}$.

The galactic rotation was investigated by the method of optical long-slit (in linear cuts) spectroscopy and in the 21 cm H I line with the WSRT radio interferometer (Rhee and Van Albada 1996). In the optical wavelength range, the stellar rotation was measured by Simien and Prugniel (2002) at a position angle of 11° and the ionized gas rotation was measured by Márquez et al. (2002) at a position angle of 90°. Both line-of-sight velocity curves rapidly reach a plateau as one recedes from the center. The stellar velocity dispersion measurements by Simien and Prugniel (2002) show that the stellar disk is dynamically very cold ($\sigma_{*,\mathrm{los}} < 50$ km s$^{-1}$) at distances of $\sim 20″$ from the center. Thus, neglecting the correction for the asymmetric drift due to the stellar disk being dynamically cold and assuming the gas and stars to rotate in the same plane, we can determine the orientation parameters of the rotation plane in space by confronting the two rotation curves. Assuming, following Erwin (2005), that the inclination of the plane to the line of sight is 48°, we

find the orientation of the dynamical line of nodes: $\mathrm{PA}_{\mathrm{dyn}} = 80°$. This is in good agreement with the orientation of the photometric major axis ($\mathrm{PA}_0 = 83°$, Erwin 2005), which confirms our assumption about a general circular rotation of NGC 7177 outside the visible bar. The rotation velocity of the galaxy in the inner stellar disk estimated for these orientation parameters is about 185 km s$^{-1}$.

In this paper, we investigate the structure, stellar population, and star formation history in the central region of NGC 7177 based on the observational data that we obtained with the Multi-Pupil Fiber Spectrograph of the 6-m telescope. According to present views, it is in the central regions of disk galaxies that the main consequences of secular evolution, in particular, the results of the matter redistribution in the disk on time scales of 1−5 Gyr governed by the effect of a nonaxisymmetric bar potential, should be sought.

## OBSERVATIONS AND DATA REDUCTION

We investigated the central region of NGC 7177 with the Multi-Pupil Fiber Spectrograph (MPFS) of the 6-m Special Astrophysical Observatory (SAO) telescope in September 2008. The MPFS (Afanasiev et al. 2001), the entrance into which is structurally made of an array of square lenses with a total size of $16 \times 16$ elements, allows the spectra from 256 spatial elements to be simultaneously taken at a scale of 1″ per lens. The galaxy was observed twice: on September 5 in the green spectral range (4200−5600 Å) at a seeing (spatial resolution) of 1″.5 and on September 7 in the red spectral range (5800−7200 Å) at a seeing better than 1″.2. Numerous emission lines of ionized gas ([O I], [O II], [O III], [N II], [S II], Hα, and Hβ) and absorption features typical of the old stellar population in galaxies fell within the spectral ranges being studied. The spectral resolution was about 3 Å. The detector was a $2048 \times 2048$-pixel CCD array.

For the primary observational data reduction, we used a software package developed at SAO and running in the IDL environment (Afanasiev et al. 2001). This package used the comparison spectrum of a gasfilled lamp to calibrate the wavelength scale and the exposure of a flat-field lamp and the twilight sky spectrum to correct the data for vignetting and different microlens transmissions.

The array (cube) of galactic spectra in the green spectral range was designed to measure the Hβ, Mgb, Fe 5270, and Fe 5335 absorption lines over the field using the recipes of the well-known Lick system (Worthey et al. 1994), the so-called Lick indices. The indices expressed as the equivalent widths of the Hβ,

Mgb, Fe 5270, and Fe 5335 absorption lines were calculated from each spectrum and were then collected into "maps". Since for these strong absorption lines there exist detailed calculations based on evolutionary synthesis models for an old stellar population (see, e.g., Worthey 1994; Thomas et al. 2003), the mean parameters of the stellar population can be estimated by comparing the observed Lick indices with the model ones. We also constructed two-dimensional line-of-sight velocity and velocity dispersion fields for stars in the central galactic region. For this purpose, after the continuum subtraction and the transformation to a logarithmic wavelength scale, the spectrum of each spatial element was cross-correlated with the spectra of the defocused (to fill the entire MPFS field of view) G9 subgiant star HD 188512 observed on the same night and with the same instrumentation as the galaxy. The observations of NGC 7177 both in the red spectral range ((5800−7200 Å), based on H$\alpha$ and [N II] $\lambda$6583), and in the green one (4200−5600 Å), containing [O III] $\lambda$5007, were used to analyze the ionized gas kinematics. We used a Gaussian fitting of the profiles for the main emission lines to construct the distributions of their surface brightnesses, line-of-sight velocities, and widths.

According to our estimates, the accuracy of individual line-of-sight velocity measurements is about $10$ km s$^{-1}$ and the accuracy of determining the equivalent widths of absorption lines at the galactic center is $\sim$0.15 Å. We checked the spectrum linearization accuracy and the zero point of the measured velocities based on the night-sky [O I] $\lambda$5577 Å and [O I]$\lambda$6300 Å lines.

NGC 7177 has been repeatedly observed with a high spatial resolution on the Hubble Space Telescope (HST) imaging cameras; we retrieved these data from the HST archive and used them in our analysis. On July 7, 2001, the galactic center was imaged with the WFPC2 camera through the $F$606$W$ and $F$814$W$ filters as part of a program aimed at searching for supernova progenitors (P.I.S. Smartt, PropID 9042). On September 19, 1997, the central region of NGC 7177 was observed with the NICMOS2 infrared camera through the $F$110$W$ and $F$160$W$ filters as part of M. Stiavelli's program (PropID 7331). The color maps constructed from these data are similar to the $R$−$I$ and $J$−$H$ colors in the optical and infrared ranges, respectively. We will use these maps in discussing the morphology of the dust distribution in the central region of NGC 7177.

## IONIZED GAS KINEMATICS AND MORPHOLOGY

Using our two-dimensional spectroscopy for the central region of NGC 7177, we constructed maps of the intensity distribution for the strongest emission lines. These are presented in Fig. 2 in arbitrary units along with the "green" and "red" continuum maps. The difference between the surface brightness distributions of the hydrogen and low-excitation (nitrogen and sulfur) lines is immediately apparent: whereas the nitrogen and sulfur emission is strongest in the galactic nucleus, the H$\alpha$ emission concentrates mainly in three compact emission-line regions located on different sides of the galactic center at distances from $1''.5$ to $2''$. Interestingly, the high-excitation [O III] $\lambda$5007 line "traces" the same three compact regions where the Balmer emission peak is observed. It should be noted that the central region of NGC 7177 was previously mapped through a narrow filter centered at the H$\alpha$ emission line and the galaxy's map in this emission line was published by Díaz et al. (2000) and Sánchez-Portal et al. (2000). Our data morphologically agree with the published ones: the same three compact H II regions that surround the nucleus of NGC 7177 are seen in Fig. 1 from Díaz et al. (2000) and Fig. 7 from Sánchez-Portal et al. (2000). Figure 3 shows the [N II] $\lambda$6583/H$\alpha$ and [O III] $\lambda$5007/H$\beta$ ratios for the various galactic regions that we distinguished. As is well known, the H$\alpha$/[N II] $\lambda$6583 ratio can serve as a diagnostic of the ionized gas excitation mechanism: this ratio is larger than unity when the gas is excited by radiation from young stars, while active nuclei exciting the gas by a nonthermal source and shocks produce a stronger nitrogen line (see, e.g., Veilleux and Osterbrock 1987). In Fig. 3, where we compare the ratios of the emission line fluxes measured in five compact regions with the theoretical calculations by Kewley et al. (2001), we see that the [N II] $\lambda$6583/H$\alpha$ ratio is large enough for the shocks or the active nucleus to be considered the prevailing gas excitation mechanism only in the nucleus of NGC 7177 itself. In the remaining circumnuclear knots and on the periphery of the region being investigated, northward and southeastward of the nucleus, the gas excitation is diagnosed either as "pure" ongoing star formation or as boundary excitation between an H II region and a shock. Obviously, we see ongoing star formation in the regions arranged in the form of a ring at $2''$ from the center of NGC 7177 and further southward, while the gas excitation mechanism in the galactic nucleus itself bears no relation to young stars.

Figure 4 presents kinematic information for the central part of NGC 7177: the maps of the ionized gas line-of-sight velocities measured from the positions of the [N II] $\lambda$6583 emission line center, the stellar line-of-sight velocities, and the velocity dispersions of gas clouds and stars. The stellar component show a cylindrical rotation within the investigated region
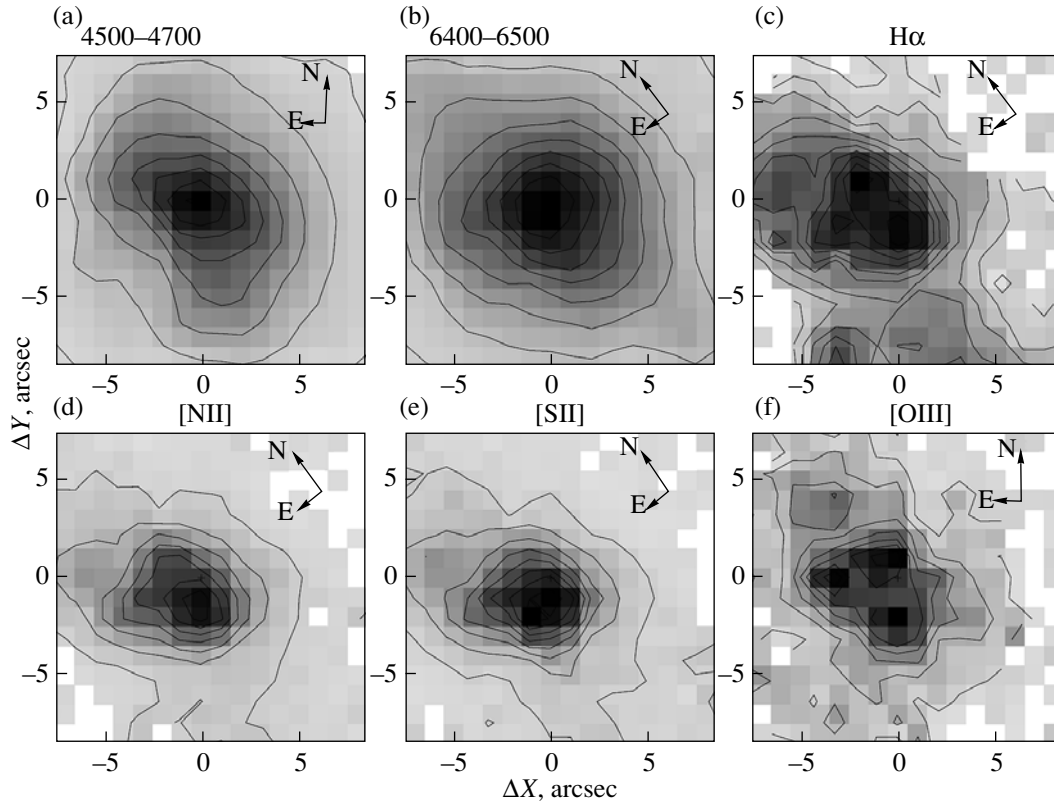
**Fig. 2.** Continuum and emission line surface brightness distributions from MPFS data: (a) continuum in the wavelength range 4500−4700 Å, (b) continuum in the wavelength range 6400−6500 Å, (c) Hα, (d) [N II] λ6583 Å, (e) [S II] λ6716 Å, and (f) [O III] λ5007 Å. The fluxes are normalized in arbitrary units.
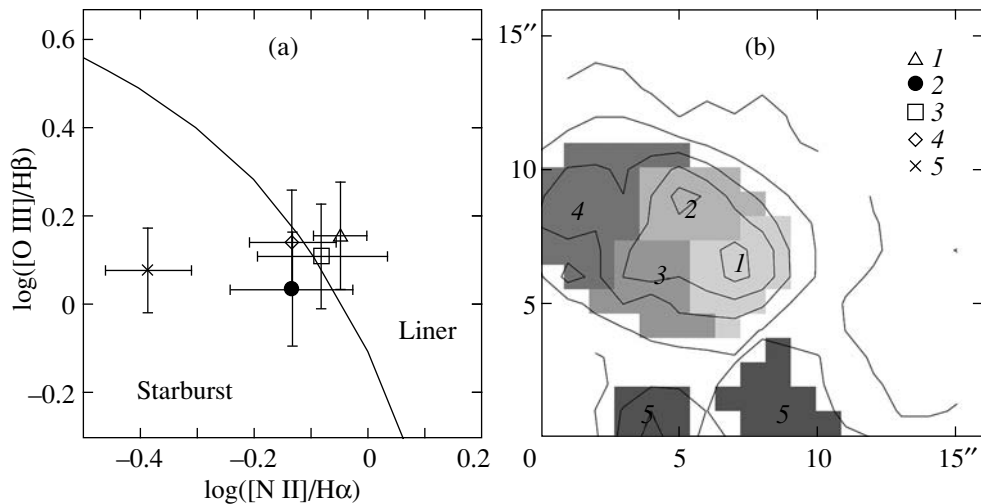


**Fig. 3.** (a) Ionization diagnostic diagram for compact regions at the center of NGC 7177; the boundary between the gas excitation by young stars and active nuclei (shocks) is shown according to the model calculations by Kewley et al. (2001); panel (b) corresponding to the MPFS field of view shows a mask that separates out the knots being studied with isophotes in the Hα emission line superimposed on the map.

whose dynamical major axis, $PA_{0,kin} = 91°$, nevertheless, deviates noticeably from the orientation of the line of nodes of the galaxy's symmetry plane

$(PA_{0,lon} = 80°)$. Bearing in mind that the galactic bar is oriented at $PA_b = 13°−18°$ (de Jong 1996), i.e., the dynamical major axis of the stellar component
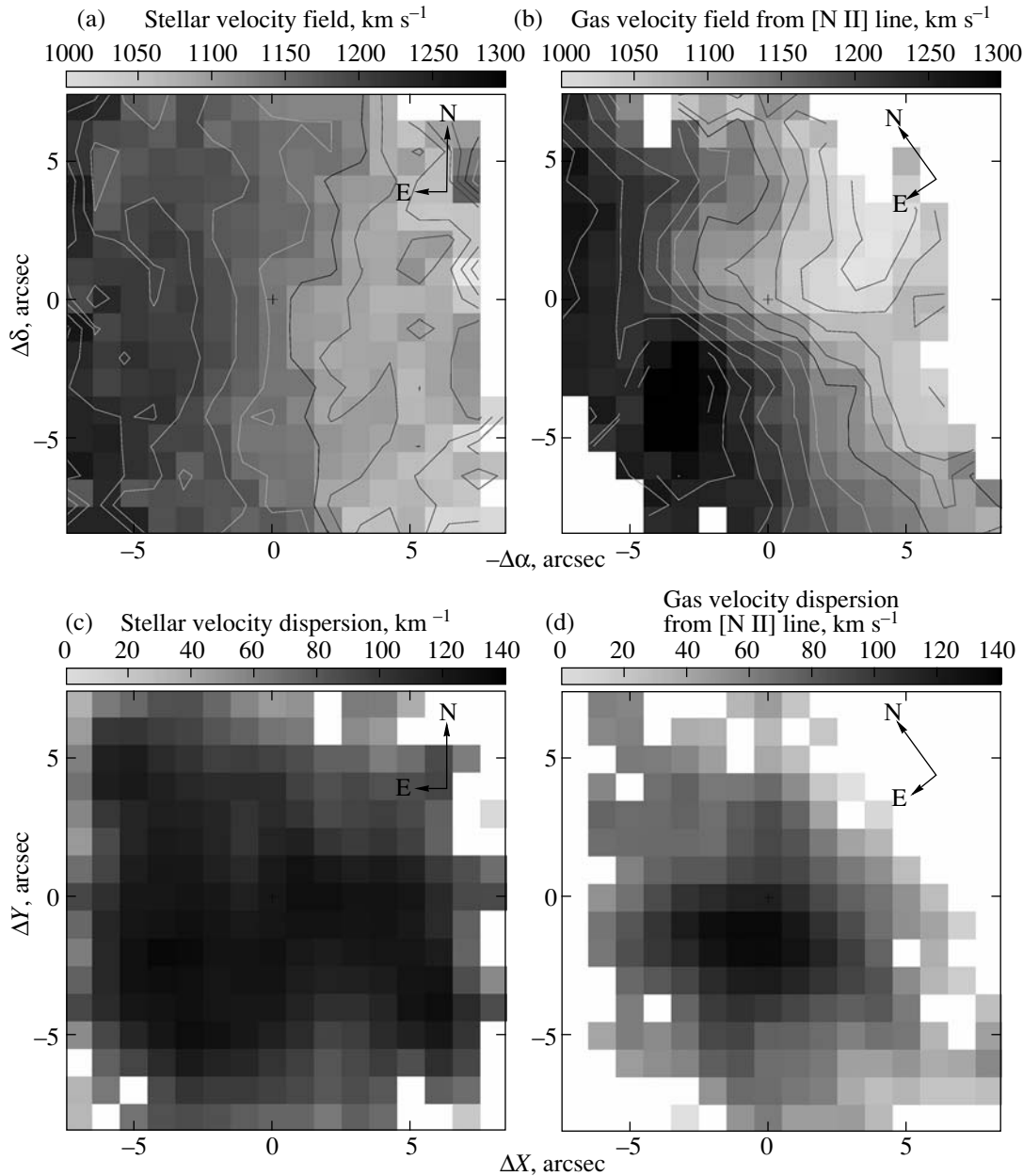
**Fig. 4.** Kinematic maps for NGC 7177 from MPFS data: (a) stellar line-of-sight velocity field (isovels + shades of gray), the line-of-sight velocities are given in km s$^{-1}$; (b) ionized gas line-of-sight velocity field (isovels + shades of gray) measured from the position of the [N II] $\lambda$6583 emission line centroid; (c) the shades of gray represent the stellar velocity dispersion; (d) the shades of gray represent the velocity dispersion of ionized gas clouds estimated from the [N II] $\lambda$6583 line width.

deviates from the orientation of the line of nodes in a direction opposite to the deviation of the isophote orientation, it can be surmised that we see the influence of a nonaxisymmetric bar potential on the regular stellar rotation. The kinematic behavior of the ionized gas differs significantly from that of the stars. The isolines of the gas line-of-sight velocity field turn noticeably within our field of view: the orientation of the kinematic major axis of the ionized gas changes from $PA_{0,kin} = 109°$ at the very center of NGC 7177 to $PA_{0,kin} = 80°$ at distances from the center larger than $4''$. Bearing in mind the orientation of the line of nodes of the global galactic disk ($PA_{0,lon} = 80°$), we may conclude that the ionized gas line-of-sight velocity distribution *within R = 4''* is most likely affected by radial motions. Thus, one might expect the gas inflow toward the galactic center in the bar potential.

The stellar velocity dispersion over the field being investigated varies insignificantly between 90 and 140 km s$^{-1}$, showing an overall elongation of the
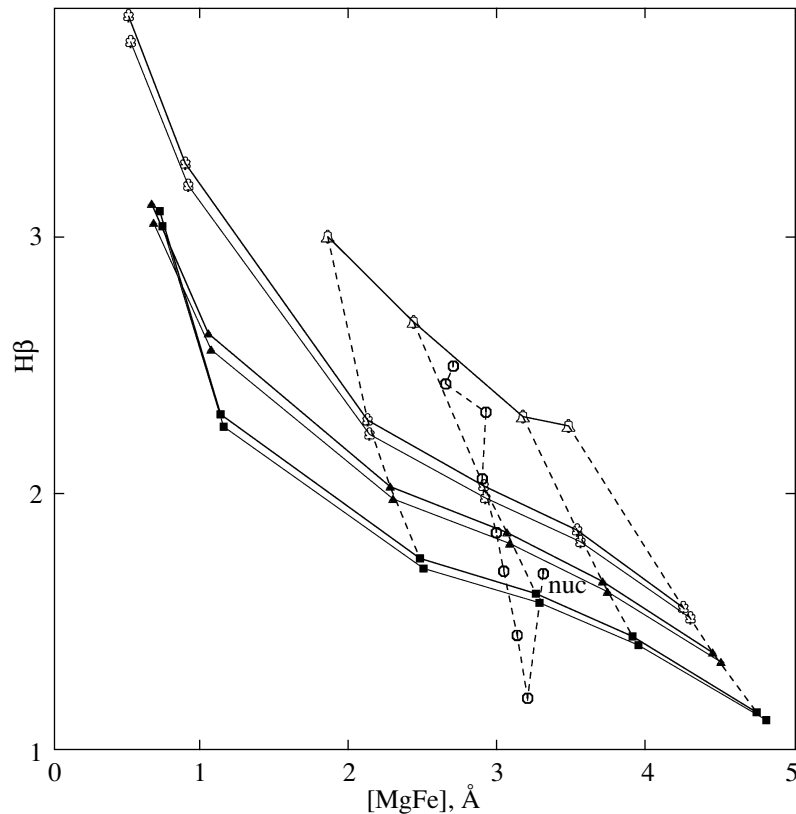
**Fig. 5.** Diagnostic diagram confronting the combined index of metal absorption lines (see the text) and the index of the Balmer H$\beta$ absorption line to determine the mean age of the stellar population. The large circles joined by the polygonal line represent the azimuthally averaged measurements of the indices in NGC 7177 taken along the radius at $1''$ steps; the galactic nucleus ($r = 0''$) is marked by **nuc**. The measurements of the H$\beta$ index were corrected for the emission as described in the text. The observational data are compared with the models from Thomas et al. (2003) for two magnesium-to-iron abundance ratios, [Mg/Fe] = 0.0 (gray polygonal line) and +0.3 (black polygonal line). The model sequences of equal age (solid lines) correspond to $T = 2, 5, 8, 12$ Gyr (from top to bottom), while the model sequences of equal metallicity (dashed lines) correspond to [Z/H] = +0.67, +0.3, 0.0, −0.33 (from right to left; for ages of 5−12 Gyr, metallicities of −1.35 and −2.35 are also marked by separate symbols).

region of maximum in the bar direction; such a behavior is in agreement with the predictions of dynamical models for the evolution of stellar bars (Vauterin and Dejonghe 1997). The local stellar velocity dispersion minima can be felt in two of the three central star-forming regions; this is natural, given the "cooling" influence of the young stars that have recently been formed out of a dynamically cold gas on the dynamics of stellar systems. The emission line widths are at a maximum in the galactic nucleus—here, the velocity dispersions of the stars and gas clouds are comparable. Outside the nucleus, the gas is a dynamically cold subsystem.

## THE AGE OF THE STELLAR POPULATION

We estimated the stellar population parameters at the center of NGC 7177 and their variations along the radius using the Lick indices H$\beta$, Mgb, and $\langle \text{Fe} \rangle \equiv (\text{Fe } 5270 + \text{Fe } 5335)/2$. To keep a constant signal-to-noise ratio with increasing distance from the nucleus, we summed the MPFS spectra of the spatial elements in rings centered on the nucleus with radii of $1'', 2'', \ldots, 8''$ and measured the indices in the summed spectra. For such a procedure, the accuracy of measuring the indices is approximately the same for all rings; at our signal-to-noise ratio, it is approximately equal to 0.15 Å. Comparison of the indices Mgb and $\langle \text{Fe} \rangle \equiv (\text{Fe } 5270 + \text{Fe } 5335)/2$ revealed a moderate magnesium overabundance with respect to iron at the center of NGC 7177: [Mg/Fe] $\approx$ +0.1. To avoid biased age estimates for the stellar population unavoidable at a nonsolar heavy-element abundance ratio if H$\beta$ is compared with the index of some element, we use a combined metal index [MgFe] $\equiv (\text{Mgb}\langle \text{Fe} \rangle)^{1/2}$ in our diagnostics. In Fig. 5, we compare our measurements of H$\beta$ and [MgFe] $\equiv (\text{Mgb}\langle \text{Fe} \rangle)^{1/2}$ with the models by Thomas et al. (2003) for [Mg/Fe] = 0.0 and +0.3. We see that

the age estimates depend weakly on the magnesium-to-iron ratio when the combined metal index is used. Figure 5 plots the values of H$\beta$ corrected for the emission that is clearly seen over the entire field of view in the central part of NGC 7177.

We made this correction by using our measurements in the red spectral range for the equivalent width of the H$\alpha$ emission line. In our view, this is the most accurate method, because there exist physical models for the relationship between the H$\alpha$ and H$\beta$ emission line intensities and because the intensity of the H$\alpha$ emission line is always several times higher than that of the H$\beta$ one, while the equivalent width of the H$\beta$ absorption line is generally of the order of or larger than that of the H$\alpha$ one. The H$\alpha$/H$\beta$ emission line ratio is smallest, 2.5–2.7 (Burgess 1958), in the case of hydrogen excitation (ionization) by ultraviolet radiation from young massive stars (H II region-type excitation). In active nuclei and shock fronts, this ratio is more than three due to the excitation mechanism itself—by a shock or photoionization by radiation with a power-law spectrum; a noticeable presence of dust in the emitting region also increases this ratio. The observational statistics including the spectra of spiral galaxies with various types of excitation gives a sample-averaged ratio EW(H$\beta$ emis) = 0.25EW(H$\alpha$ emis) (Stasinska and Sodré 2001). As we ascertained in the previous section, individual star-forming regions are observed at the center of NGC 7177 against the general background of shock excitation of the emission-line spectrum. In the spectra of the red region summed in the rings, the nitrogen emission line is stronger than the H$\alpha$ emission line at all distances from the center. Therefore, correcting the index H$\beta$ for the emission in the central region of NGC 7177, we will take EW(H$\beta$ emis) = 0.25EW(H$\alpha$ emis) in all rings within 8$''$ of the center.

We see on the diagnostic diagram in Fig. 5 that the galactic nucleus is old, with a mean stellar population age of ~10 Gyr. As one recedes from the center, the mean stellar population age decreases and reaches a constant value of ~2−3 Gyr starting from a radius of ~6$''$. The mean stellar metallicity is almost constant along the radius, being approximately solar.

## DISCUSSION

The morphology of the central region in NGC 7177 has been repeatedly studied using data from the HST, which provided the galaxy's images in various spectral bands, from the ultraviolet to near-infrared ones, with a high spatial resolution. The central region of the galaxy is rich in dust, whose distribution at the center of NGC 7177 is characterized in the literature as "extremely chaotic" (González Delgado

et al. 2008). Figure 6 presents the $F110W-F160W$ infrared color map for the central region of NGC 7177 that we constructed from NICMOS/HST data (the spatial resolution is 0$''$.2)—this color band is close to $J-H$. The map was turned so as to correspond in orientation to the field exposed for NGC 7177 with MPFS/BTA in the red spectral range. We see that the dust at the center of NGC 7177 is optically thick: it is clearly traceable in the form of red lanes southeastward of the nucleus even in the infrared color. The $F606W-F814W$ (WFPC2/HST) color map (not shown here) demonstrates the same morphology. However, we would not classify the dust distribution at the center of NGC 7177 as chaotic; on the contrary, the dust lanes extend quite orderly along the southern "leading" edge of the bar. As the center is approached, within a radius of ~4$''$, the dust lane turns almost though a right angle and crosses the nucleus at PA $\approx 70°$. Such a morphology of the dust distribution is well reproduced in the dynamical models of the "response" of a gaseous disk to a rotating bar if the bar has a double inner Lindblad resonance and is explained by the structure of the shock fronts in the gas flowing on the bar (Athanassoula 1992). However, in this case, only "half" of the bar shock fronts is seen in NGC 7177; a symmetric extension of the dust pattern northward of the nucleus should be expected in the theory. If we grasp that the galactic disk is inclined approximately at 50° to the plane of the sky and that the southern side of the disk is nearest to us (in order that the southeastern edge of the bar be the leading one), then the absence of the northern dust lane on the color maps can mean only one thing: the bar in NGC 7177 is vertically thick and screens the shock front in the thin gaseous disk northwestward of the nucleus. A photometric analysis of the surface brightness profile shows that the bulge in the galaxy is compact and it dominates over the disk at galactocentric distances $R < 8''$ (Baggett et al. 1998) − $R < 15''$ (Graham 2001); i.e., the bar in NGC 7177 with a semimajor axis of only 10$''$−13$''$ (de Jong 1996; Erwin 2005) is a structure of the bulge rather than the disk and, in a sense, it is the bulge itself or, more precisely, a "pseudo-bulge" whose formation mechanism can be dynamical bar heating perpendicular to the disk plane (Chung and Bureau 2004).

According to the model results by Athanassoula (1992), the change in the orientation of the dust lanes as the center is approached is evidence for the presence of a double inner Lindblad resonance in the bar. As we made sure above, the H$\alpha$ emission is located around the nucleus in the form of knots at equal distances of 1$''$.5−2$''$, which can be characterized as an inhomogeneous nuclear star formation
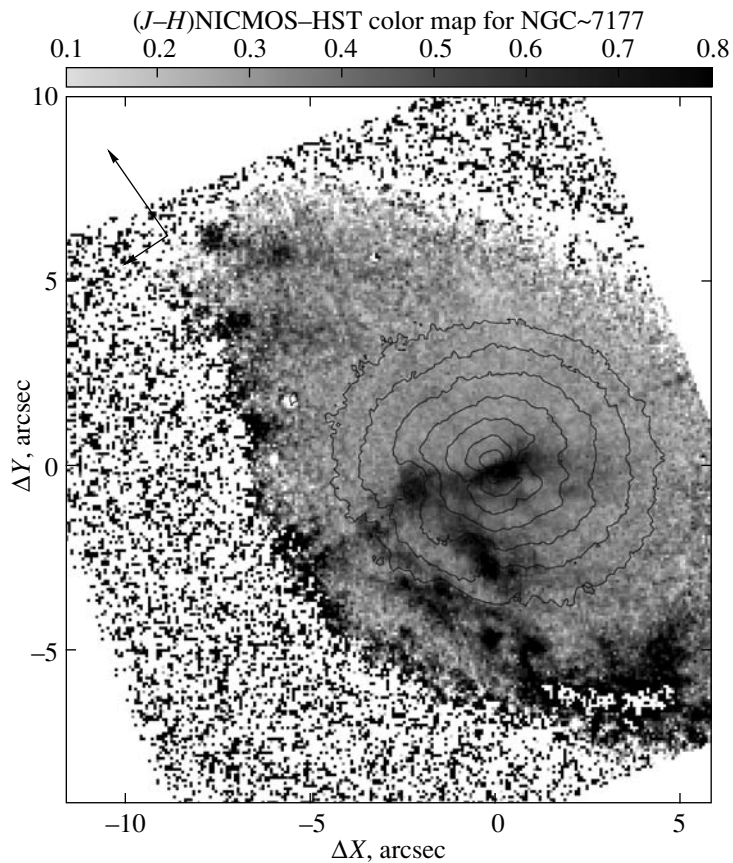
**Fig. 6.** $F110W - F160W$ $(J - H)$ color map for the central region of NGC 7177 from NICMOS/HST data. The color zero point is arbitrary.

ring. The nuclear star formation rings are also usually associated with the inner Lindblad resonances of the bars (Buta and Crocker 1993) and theoreticians place them between the inner inner and outer inner Lindblad resonances (Heller and Shlosman 1996). Can we estimate the possible locations of the inner Lindblad resonances in NGC 7177? As we mentioned in the Introduction, the galactic rotation curve was measured by Márquez et al. (2002) from the ionized gas; in the Introduction, we also refined the orientation of the line of nodes for NGC 7177. Having calculated the circular rotation curve in the galactic plane from the data by Márquez et al. (2002), we made sure that it demonstrates a local maximum at a galactocentric distance $R \approx 5''$. Figure 7 presents this rotation curve in angular units of km s$^{-1}$ arcsec$^{-1}$ (solid curve) and the dependence on radius for $\Omega - \kappa/2$ (dashed curve). The intersection of the latter curve with the constant at the level of the bar pattern speed gives the position of the inner Lindblad resonance. If there is a fast bar in NGC 7177 typical of early-type spiral galaxies (Rautiainen et al. 2008), then the ratio of the corotation radius to the bar radius is 1.0−1.4. The

upper boundary of this ratio places the inner inner Lindblad resonance in NGC 7177 at $R \approx 2''$ precisely where the star formation ring is observed. So, the set of kinematic and morphological data is consistent with the standard model picture of the gas motion and the dust distribution between the two inner Lindblad resonances at the center of NGC 7177.

The mean stellar age inside the star formation ring in the galactic nucleus is ∼10 Gyr. Outside the star formation ring, at a distance $R = 6'' - 8''$ from the nucleus, the mean age of the stellar population is ∼2 Gyr. The dynamical and morphological signatures suggest that the bar in NGC 7177 is old: it has managed to thicken in $z$ coordinate and the stellar velocity dispersion in the galactic center is at a maximum, which is also indicative of an advanced stage of dynamical evolution. If the bar lifetime and the mean stellar population age at the outer inner Lindblad resonance are comparable, then it can be surmised that the star formation ring has migrated radially inward in the last 1−2 Gyr; such a behavior of the nuclear star formation rings is actually observed in barred galaxies (see the Introduction in van de Ven
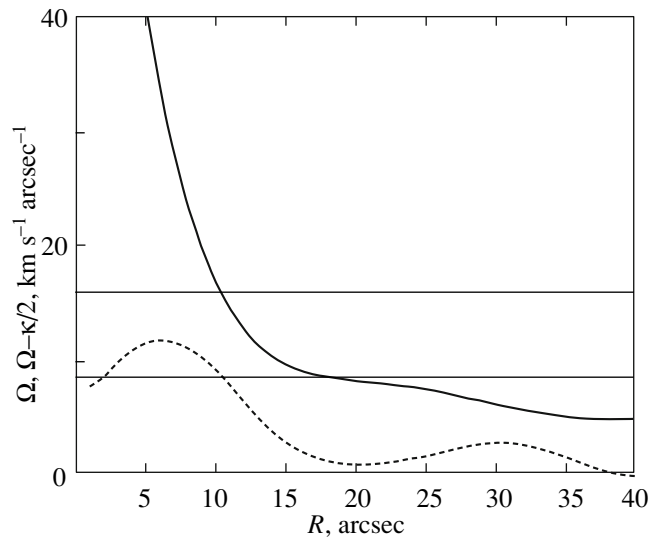
**Fig. 7.** Rotation curve in the central region of NGC 7177 based on data from Márquez et al. (2002) and positions of the inner Lindblad resonances; the interval for the angular velocity of the bar denoted by the thin horizontal solid lines is taken according to the assumption that the bar in NGC 7177 is fast.

and Chang (2009)) and is predicted by various dynamical models of nuclear resonant rings (Regan and Teuben 2003; van de Ven and Chang 2009). This wave of star formation (and gas concentration) has not yet reached the nucleus and as yet there have been no chances for the supermassive black hole at the center of NGC 7177, if it exists, to become a truly active nucleus.

## ACKNOWLEDGMENTS

## REFERENCES

1. V. L. Afanasiev, S. N. Dodonov, and A. V. Moiseev, in *Stellar Dynamics: From Classic to Modern,* Ed. by L. P. Osipkov and I. I. Nikiforov (SPb. Gos. Univ., St.-Petersbourg, 2001), p. 103.
2. E. Athanassoula, Mon. Not. R. Astron. Soc. **259**, 345 (1992).
3. W. E. Baggett, S. M. Baggett, and K. S. J. Anderson, Astron. J. **116**, 1626 (1998)
4. A. Burgess, Mon. Not. R. Astron. Soc. **118**, 477 (1958).
5. R. Buta and D. A. Crocker, Astron. J. **105**, 1344 (1993).
6. A. Chung and M. Bureau, Astron. J. **127**, 3192 (2004).
7. A. I. Díaz, M. Alvarez Alvarez, E. Terlevich, et al., Mon. Not. R. Astron. Soc. **311**, 120 (2000).
8. P. Erwin, Mon. Not. R. Astron. Soc. **364**, 283 (2005).
9. P. Erwin, M. Pohlen, and J. E. Beckman, Astron. J. **135**, 20 (2008).
10. R. M. González Delgado, E. Pérez, R. Cid Fernandez, and H. Schmitt, Astron. J. **135**, 747 (2008).
11. A. W. Graham, Astron. J. **121**, 820 (2001).
12. C. H. Heller and I. Shlosman, Astrophys. J. **471**, 143 (1996).
13. R. S. de Jong, Astron. Astrophys. Suppl. Ser. **118**, 557 (1996).
14. L. J. Kewley, M. A. Dopita, R. S. Sutherland, et al., Astrophys. J. **556**, 121 (2001).
15. J. Kormendy and R. C. Kennicutt, Jr., Ann. Rev. Astron. Astrophys. **42**, 603 (2004)
16. I. Márquez, J. Masegosa, M. Moles, et al., Astron. Astrophys. **393**, 389 (2002).
17. K. A. Misselt, G. C. Clayton, and K. D. Gordon, Publ. Astron. Soc. Pacific **111**, 1398 (1999).

18. P. Rautiainen, H. Salo, and E. Laurikainen, Mon. Not. R. Astron. Soc. **388**, 1803 (2008).

19. M. W. Regan and P. Teuben, Astrophys. J. **582**, 723 (2003).

20. M.-H. Rhee and T. S. van Albada, Astron. Astrophys. Suppl. Ser. **115**, 407 (1996).

21. M. Sánchez-Portal, A. I. Díaz, R. Terlevich, et al., Mon. Not. R. Astron. Soc. **312**, 2 (2000).

22. F. Simien and Ph. Prugniel, Astron. Astrophys. **384**, 371 (2002).

23. G. Stasinska and I. Sodré, Jr., Astron. Astrophys. **374**, 919 (2001).

24. D. Thomas, C. Maraston, and R. Bender, Mon. Not. R. Astron. Soc. **339**, 897 (2003).

25. P. Vauterin and H. Dejonghe, Mon. Not. R. Astron. Soc. **286**, 812 (1997)

26. S. Veilleux and D. E. Osterbrock, Astrophys. J. Suppl. Ser. **63**, 295 (1987).

27. G. van de Ven and Ph. Chang, Astrophys. J. **697**, 619 (2009).

28. G. Worthey, Astrophys. J. Suppl. Ser. **95**, 107 (1994).

29. G. Worthey, S. M. Faber, J. J. Gonzalez, and D. Burstein, Astrophys. J. Suppl. Ser. **94**, 687 (1994).

*Translated by V. Astakhov*